The astrophysical reactions $^{12}C(\alpha,\gamma)^{16}O$ and $^{7}Be(p,\gamma)^{8}B$ and Coulomb dissociation experiments

C.A. Bertulani
Gesellschaft für Schwerionenforschung, KPII, Planckstrasse 1, D-64291 Darmstadt, Germany
(Received 6 December 1993; revised manuscript received 19 January 1994)

The use of the Coulomb dissociation method to obtain the cross sections for the radiative capture reactions $^{12}C(\alpha,\gamma)^{16}O$ and $^{7}Be(p,\gamma)^{8}B$ is investigated. The contribution of the nuclear interaction to the breakup is included. Due to the low binding of the proton in ^{8}B the second reaction is dominated by Coulomb breakup. The effects of Coulomb reacceleration of the fragments and of the excitation of states in the fragments are also studied. Ideal kinematical conditions for the experiments are investigated.

PACS number(s): 25.40.Lw, 25.55.−e, 97.10.Cv, 27.20.+n

I. INTRODUCTION

Among many radiative capture reactions of interest in astrophysics, the $^{12}C(\alpha,\gamma)^{16}O$ and $^{7}Be(p,\gamma)^{8}B$ reactions attract most of the experimental interest. The first reaction is a key one in the synthesis of heavier elements, linking the stage of helium burning into carbon and oxygen and the later stages of carbon and oxygen burning. The stellar burning for this reaction occurs at 300 keV. Due to the Coulomb repulsion the cross section is very small and no direct laboratory measurements have been done at this energy. This reaction is dominated by the $E1$ and $E2$ electromagnetic capture. One predicts that these two components for the radiative capture are equally important at 300 keV [1]. Recently indirect experiments have been done by measuring the β-delayed α decay of ^{16}N which allowed the determination of the $E1$ component of the radiative capture cross section [2, 3]. As for the $E2$ component another alternative experiment has yet to be found to finally determine the value of the radiative cross section at 300 keV.

An alternative is the Coulomb dissociation method. It has been proposed in Ref. [4]. The method is based on the fact that the dissociation of a projectile in the Coulomb field of a heavy target can be directly related to the photodissociation cross section. This method has been successful in determining the radiative capture cross sections of the reactions $^{13}N(p,\gamma)^{14}O$ [5] and $^{2}H(\alpha,\gamma)^{6}Li$ [6].

It can be shown that the Coulomb induced $E2$ excitations are larger than the $E1$ excitations at low bombarding energies ($\sim$ 50 MeV/nucleon) [7]. Exploring this property a recent study on the use of this method for $^{12}C(\alpha,\gamma)^{16}O$ has been performed in Ref. [8]. The contribution of the nuclear interaction to the breakup was neglected. In Sec. III of this work we study the effects of the nuclear induced breakup. It is shown to be important and makes it very difficult to disentangle the nuclear from the Coulomb induced breakup.

The other reaction of great interest in astrophysics is $^{7}Be(p,\gamma)^{8}B$. It is closely related to the so-called solar neutrino problem [9]. The radiative capture cross section has been measured to relative energies as low as 150 keV. But in the Sun the reaction occurs at a much lower energy, $E_{p\text{-}Be} = 20$ keV. The possibility for a direct measurement at this energy is currently nonexistent, due to the very small cross section. The Coulomb dissociation method offers a good alternative. As shown in Sec. IV of this work the breakup cross section is dominated by the Coulomb dissociation mechanism at intermediate bombarding energies.

A difficulty in these experiments is the precise determination of the breakup energy. This will be considered in Sec. V. It is shown that under normal conditions an accuracy of 20 keV is obtainable. But before we proceed it is important to show how to relate the coincidence measurements obtained in Coulomb breakup experiments with the radiative capture cross section for a given energy. This is done in Sec. II.

II. DETERMINING THE RADIATIVE CAPTURE CROSS SECTIONS FROM COULOMB BREAKUP

To relate the cross section for the Coulomb breakup $a + A \longrightarrow b + c + A$ with the astrophysical S factors relevant for the reaction $b + c \longrightarrow a + \gamma$ what is needed is the cross section

$$\frac{d^3\sigma}{dE_b\, d\Omega_b\, d\Omega_c}\,. \tag{1}$$

The relative motion energy E_{bc} and the laboratory energy $E_{\rm lab}$ are related to the measured values of the final energies of the fragments, E_b and E_c, respectively, by

$$E_{bc} = E_x + Q = \frac{p_{bc}^2}{2m_{bc}}$$
$$\text{and} \qquad E_b + E_c = E_{\rm lab} + Q - E_{\rm recoil}\,, \tag{2}$$

where E_x is the energy transfer to the system $b + c$ and

$$\mathbf{p}_{bc} = m_{bc}\left(\frac{\mathbf{p}_b}{m_b} - \frac{\mathbf{p}_c}{m_c}\right) \qquad \text{and} \qquad m_{bc} = \frac{m_b m_c}{m_a}\,; \tag{3}$$

The binding energy of $b+c$, and the recoil energy of the target are given by Q and $E_{\rm recoil}$, respectively. We consider a lead target due to its large charge. For ^{8}B projectiles, $Q=-140$ keV, while for ^{16}O, $Q=-7.162$ MeV. The lead target is assumed to remain in its ground state. At bombarding energies around (or higher than) some tens of MeV per nucleon, a simple recoil formula can be derived as a function of the scattering angle. The recoil energy arises from the Coulomb repulsion and is given by

$$E_{\rm recoil} \approx \frac{(Z_a Z_A e^2)^2}{(m_A/m_a)E_{\rm lab}\, b^2}\,. \tag{4}$$

As an example we take the impact parameter b as 15 fm, in the reaction ^{8}B+^{208}Pb. Then $E_{\rm recoil}\approx 250$ keV, at $E_{\rm lab}=240$ MeV (30 MeV/nucleon). From these numbers we see that for this particular reaction

$$Q,\ E_{\rm recoil} \ll E_{\rm lab}\,.$$

Thus, the projectile energy is basically the same before and after the breakup.

Calling by Ω_{bc} the relative solid angle of the $(b+c)$ system in their c.m. frame, E_{bc} their relative energy in this frame, and Ω_a the scattering angle of the $a+A$ system, we have the relationship

$$\frac{d^4\sigma}{dE_{bc}\,dE_T\,d\Omega_{bc}\,d\Omega_a} = \frac{d^4\sigma}{dE_b\,dE_c\,d\Omega_b\,d\Omega_c}\,J\,, \tag{5}$$

where $E_T=E_c+E_b-Q+E_{\rm recoil}$ is the total kinetic energy and J is the Jacobian

$$J=\frac{\partial(E_b,\,E_c,\,\Omega_b,\,\Omega_c)}{\partial(E_{bc},\,E_T,\,\Omega_{bc},\,\Omega_a)}=\frac{m_{bc}\,p_{bc}\,M_{aA}\,p_R}{m_b\,p_b\,m_c\,p_c}\,, \tag{6}$$

where

$$M_{aA}=\frac{m_a\,m_A}{m_a+m_A}$$

and

$$\mathbf{p}_R=\frac{m_a}{m_a+m_A}\mathbf{P}_{\rm lab}-\mathbf{p}_b-\mathbf{p}_c\,. \tag{7}$$

We use now energy conservation, multiplying Eq. (5) by $\delta(E_T-E_{\rm lab})$ and integrate it over E_c. We get

$$\frac{d^3\sigma}{dE_b\,d\Omega_b\,d\Omega_c}=\frac{m_b\,p_b\,m_c\,p_c}{m_{bc}\,p_{bc}\,M_{aA}\,p_R}\,\frac{d^3\sigma}{dE_{bc}\,d\Omega_{bc}\,d\Omega_a}\,\frac{\partial E_c}{\partial E_T}\,, \tag{8}$$

where the relation between the variables are given by Eqs. (2), (3), and (7), and

$$\frac{\partial E_c}{\partial E_T}=m_A\left[m_c+m_A-m_c\frac{\mathbf{p}_c\cdot(\mathbf{p}_R-\mathbf{p}_b)}{p_c^2}\right]^{-1} \tag{9}$$

In order to relate the cross section $d^3\sigma/dE_b\,d\Omega_b\,d\Omega_c$ with the astrophysical S factors we assume for simplicity that the angular distribution of the fragments is isotropic in the projectile frame of reference. This approximation is not necessary. As shown in Ref. [10] one can calculate the angular correlations between the fragments for a given experimental condition. We get

$$\frac{d^3\sigma}{dE_b\,d\Omega_c\,d\Omega_b}=\frac{m_b\,p_b\,m_c\,p_c}{4\pi\,m_{bc}\,p_{bc}\,M_{aA}\,p_R}\,\frac{\partial E_c}{\partial E_T}\,\frac{d^2\sigma}{dE_{bc}\,d\Omega_a}\,. \tag{10}$$

The relation with the photodissociation cross section is obtained by using [4]

$$\frac{d^2\sigma}{dE_{bc}\,d\Omega_a}=\frac{d^2\sigma}{dE_x\,d\Omega_a}=\frac{1}{E_x}\,\frac{dn_{\pi\ell}}{d\Omega_a}\,\sigma(\gamma+a\longrightarrow b+c)\,, \tag{11}$$

where $dn_{\pi\ell}/d\Omega_a$ is the virtual photon number per unit solid angle Ω_a, for the relevant $\pi\ell$ multipolarity in the breakup process. The photodissociation cross section can be related to the radiative capture cross section by means of the detailed balance theorem. One obtains finally

$$\frac{d^3\sigma}{dE_b\,d\Omega_c\,d\Omega_b}=\frac{m_b\,p_b\,m_c\,p_c}{m_{bc}\,p_{bc}\,M_{aA}\,p_R}\,\frac{\partial E_c}{\partial E_T}\,\frac{(2J_b+1)\,(2J_c+1)}{4\pi\,(2J_a+1)}\,m_{bc}c^2\,\frac{dn_{\pi\ell}}{d\Omega_a}\,\frac{S(E_{bc})}{E_x^3}\,\exp\left[-\frac{2\pi Z_b Z_c e^2}{\hbar}\sqrt{\frac{m_{bc}}{2E_{bc}}}\right]. \tag{12}$$

Semiclassical expressions for the virtual photon numbers are given, e.g., in Ref. [7]. These were used in Ref. [8] to deduce the relative contribution of the $E2$ and $E1$ breakup mode to the reaction Pb(^{16}O,α+^{12}C)Pb. However, this reaction is strongly influenced by the nuclear interaction. The equivalent photon numbers are also influenced strongly by the distortion of the c.m. scattered wave. A way to account for this effect was given in Ref. [11].

III. COULOMB VERSUS NUCLEAR BREAKUP

As shown in Ref. [11] the Coulomb excitation amplitude in high energy collisions for a given multipolarity $E\lambda$, including the effect of strong absorption, is given by

$$f_{E1,\mu}(E_x,\theta)=i\frac{\sqrt{8\pi}}{3}\,\frac{Z_T e M_{aA}}{\hbar^2}\left(\frac{E_x}{\hbar v_a}\right)\left[B(E1,\,E_x)\right]^{1/2}\begin{cases}\Lambda_{\pm1}(E_x,\,\theta) & \text{if } \mu=\pm1,\\ \Lambda_0(E_x,\,\theta) & \text{if } \mu=0,\end{cases} \tag{13}$$

for $E1$ excitations, and

$$f_{E2,\mu}(E_x,\theta)=-\frac{2}{5}\,\frac{\sqrt{\pi}}{6}\,\frac{Z_T e M_{aA}}{\hbar^2}\left(\frac{E_x}{\hbar v_a}\right)^2\left[B(E2,\,E_x)\right]^{1/2}\begin{cases}\Lambda_{\pm2}(E_x,\,\theta)/\gamma & \text{if } \mu=\pm2,\\ -(2-v^2/c^2)\,\Lambda_{\pm1}(E_x,\,\theta) & \text{if } \mu=\pm1,\\ \Lambda_0(E_x\,\theta) & \text{if } \mu=0\end{cases} \tag{14}$$

for $E2$ excitations. In the above equations $\gamma = (1 - v_a^2/c^2)^{-1/2}$, and μ is the azimuthal component of the transferred angular momentum. The functions Λ_μ are given by [11]

$$\Lambda_\mu(E_x,\ \theta) = \int_0^\infty db\ b\ J_\mu(qb)\ K_\mu\Big(\frac{E_x b}{\gamma\hbar v_a}\Big)\ \exp\Big[i\chi(b)\Big], \tag{15}$$

where $q = 2k\sin(\theta/2)$, k is the c.m. momentum of $a+A$, and J_μ (K_μ) are Bessel (modified) functions of order μ. $\chi(b)$ is given by

$$\chi(b) = -\frac{1}{\hbar v_a}\int_{-\infty}^{\infty} U_N^{(aA)}(z',\ b)dz' + \chi_C(b), \tag{16}$$

where $U_N^{(aA)}(r)$ is the nuclear potential for the $a + A$ system. The Coulomb phase is given by

$$\chi_C(b) = 2\frac{Z_a Z_A e^2}{\hbar v}\ \Big\{\ \Theta(b-R_0)\ \ln(kb) + \Theta(R_0-b)\ \Big[\ln(kR_0) + \ln\Big(1+(1-b^2/R_0^2)^{1/2}\Big) - (1-b^2/R_0^2)^{1/2} - \frac{1}{3}\ (1-b^2/R_0^2)^{3/2}\Big]\Big\}. \tag{17}$$

The first term inside the parentheses is the Coulomb eikonal phase for pointlike charge distributions. The second term accounts for the finite extension of the charge distributions. The radius R_0 is taken as the sum of the radii of two uniform charge distributions, $R_0 = 1.2\ (A_a^{1/3} + A_A^{1/3})$ fm.

Using the detailed balance theorem the reduced matrix elements $B(E\lambda,\ E_x)$ are given by

$$B(E1,\ E_x) = \frac{27}{64\pi^3}\ \frac{\hbar}{m_{bc}c}\ \frac{E_x}{E_{bc}^2}\ S_{E1}(E_{bc}) \times \exp\Big[-\frac{2\pi Z_b Z_c e^2}{\hbar}\sqrt{\frac{m_{bc}}{2E_{bc}}}\Big] \tag{18}$$

and

$$B(E2,\ E_x) = \frac{1125}{48\pi^3}\ \frac{\hbar^3 c}{m_{bc}}\ \frac{1}{E_{bc}^2\ E_x}\ S_{E2}(E_{bc}) \times \exp\Big[-\frac{2\pi Z_b Z_c e^2}{\hbar}\sqrt{\frac{m_{bc}}{2E_{bc}}}\Big], \tag{19}$$

where it was assumed that the transitions are from the ground state ($J = 0$) to the $J = 1$ and $J = 2$ continuum states, respectively.

The nuclear contribution to the breakup can be calculated within the distorted wave Born approximation. The breakup amplitude is

$$f_N = -\frac{M_{aA}}{2\pi\hbar^2}\ \langle\Psi^{(-)}(\mathbf{R})\phi_f(\mathbf{r})|\Delta V(\mathbf{r},\mathbf{R})|\Psi^{(+)}(\mathbf{R})\phi_i(\mathbf{r})\rangle, \tag{20}$$

where $\mathbf{r}$ is the vector between the fragments b and c and $\mathbf{R}$ is the $a+A$ relative coordinate. The coupling interaction is

$$\Delta V(\mathbf{r},\mathbf{R}) = U_N^{(bA)}(\mathbf{r}_{bA}) + U_N^{(cA)}(\mathbf{r}_{cA}) - U_N^{(aA)}(\mathbf{R}). \tag{21}$$

Above, $U_N^{(aA)}$ is the projectile-target optical potential and $U_N^{(bA)}$ and $U_N^{(cA)}$ are fragment-target optical potentials. The coordinates $\mathbf{r}_{bA}$ and $\mathbf{r}_{cA}$ are given by

$$\mathbf{r}_{bA} = \mathbf{R} - \frac{m_b}{m_a}\mathbf{r}\ , \qquad \mathbf{r}_{cA} = \mathbf{R} + \frac{m_c}{m_a}\mathbf{r}\ , \tag{22}$$

where m_i stands for the mass of particle i. In Eq. (20) $\Psi^{(+)}$ ($\Psi^{(-)}$) is the distorted wave with outgoing (incoming) boundary condition, $\phi_i(\mathbf{r})$ is the bound ground state of $b + c$, and $\phi_f(\mathbf{r})$ is the final state with the fragments in the continuum.

For the c.m. scattering waves we use the eikonal approximation

$$\Psi^{(-)*}(\mathbf{R})\Psi^{(+)}(\mathbf{R}) = \exp\Big\{i\mathbf{q}\cdot\mathbf{R} + i\chi(b)\Big\}\ , \tag{23}$$

where $\chi(b)$ is given by Eq. (16).

Since the optical potentials $U^{(aA)}$, $U^{(bA)}$, and $U^{(cA)}$ are not known experimentally for all combinations studied here, we construct them by using the "t-$\rho\rho$" approximation [12]. They are given by

$$U_N^{(jA)}(\mathbf{R}) = -\frac{\hbar v_{aA}}{2}\ \sigma_{NN}\ (\alpha+i)\ \int d^3r\ \rho_j(\mathbf{r})\ \rho_A(\mathbf{R}-\mathbf{r})\ , \tag{24}$$

where ρ_j ($j = a, b, c$) and ρ_A are the ground state densities, σ_{NN} is the nucleon-nucleon cross section, and α is the ratio between the real and the imaginary parts of the nucleon-nucleon scattering amplitude at zero degree. In Table I we give a set of values for σ_{NN} and α for three laboratory energies used here. The ground state densities of carbon, oxygen, and lead are parametrized by a modified Fermi function $\rho(r) = \rho(0)(1 + cr^2/R_0^2)\Big\{1 + \exp\Big[(r - R_0)/a\Big]\Big\}^{-1}$ and the proton by a Gaussian density. The densities are normalized to the mass number. The parameters used are given in Table II.

The transition densities, $\delta_{fi} = \phi_i\ \phi_f^*$, for these reac-

TABLE I. Parameters of the nucleon-nucleon amplitude. The amplitude is considered isotropic: $f_{NN} = k_{NN}\sigma_{NN}(\alpha + i)/4\pi$. These values are taken from [13].

$E_{\rm lab}$ (MeV/nucl)	σ_{NN} (fm^2)	α
30	19.6	0.87
50	10.3	0.94
100	5.3	1.0

TABLE II. Parameters for the nuclear ground state densities. A modified Fermi function $\rho(r) = \rho(0)(1+cr^2/R_0^2)\{1+\exp[(r-R_0)/a]\}^{-1}$ was used for carbon, oxygen, and lead. The density of the proton was parametrized by a Gaussian with radius size R_0. The data are from Ref. [14].

Nucleus	R_0	a	c
H	0.8	—	—
^{12}C	2.335	0.522	−0.149
^{16}O	2.608	0.513	0
^{208}Pb	6.624	0.549	0

tions were calculated by using a two-body model for the system $b+c$. In particular, we assume that U_{bc} is the sum of nuclear, U_N^{bc}, and Coulomb, U_C^{bc}, terms. For the former, we take a Gaussian form,

$$U_{bc} = U_0 \exp\left\{-\frac{r^2}{R_0^2}\right\}, \tag{25}$$

while for the latter we take the Coulomb potential of a homogeneously charged sphere of radius R_c:

$$U_C(r) = Z_b Z_c e^2 \times \begin{cases} 1/r & \text{for } r \geq R_c, \\ (3 - r^2/R_c^2)/2R_c & \text{for } r < R_c. \end{cases} \tag{26}$$

In the case of $^{12}C+\alpha$ we used $U_0 = -85.9$ MeV, $R_0 = 2.8$ fm, and $R_c = 3.55$ fm. These parameters yield a ground state wave function with binding energy equal to $Q = -7.16$ MeV. For $p+^7Be$ we use $U_0 = -90.5$ MeV, $R_0 = 1.9$ fm, and $R_c = 2.4$ fm, which yield a binding of $Q = -140$ keV. Although not completely legitimate, we used the same set of parameters to obtain the wave functions ϕ_f in the continuum.

The continuum wave functions are normalized to one state per unit energy. Formally this is written

$$\langle \phi_f(E) | \phi_f(E') \rangle = \delta(E - E'). \tag{27}$$

In practical terms, Eq. (27) requires that the continuum wave functions are normalized to the asymptotic form

$$\phi_f(r) \longrightarrow \sqrt{2m_{bc}/\hbar^2 \pi k}\, \frac{\sin(kr+\delta)}{r}, \tag{28}$$

$k = \sqrt{2m_{bc}E/\hbar^2}$, and δ is the phase shift. With this normalization the differential cross section is given by

$$\frac{d^2\sigma}{d\Omega_a dE_{bc}} = \left| \sum_\mu f_{E\ell,\mu} + f_N \right|^2 \tag{29}$$

For $^{16}O+Pb \longrightarrow \alpha+^{12}C+Pb$ we use $\ell = 2$ while for $^8B+Pb \longrightarrow p+^7Be+Pb$ we use $\ell = 1$, with the Coulomb amplitudes calculated as in Eqs. (13) and (14).

IV. DIFFERENTIAL CROSS SECTIONS

Here we apply the formulation of the previous section to obtain the differential cross section $d^2\sigma/dE_{bc}d\Omega_a$ which can be used as input in Eq. (10) to relate to the experimental measurements. In Fig. 1 we show the differential cross section for the breakup of ^{16}O into $\alpha+^{12}C$ in a collision with a lead target at 100 MeV/nucleon. This energy is ideal for this experiment. At lower energies the cross section is smaller. At high energies the magnitude of the cross section is somewhat larger but it is also more difficult to have a good angular resolution for the fragments due to the narrowing of the kinematical cone. A total excitation energy $E_x = 8.1$ MeV was chosen.

The Coulomb amplitude is dominated by the $E2$ multipolarity. Thus, we used Eqs. (14) and (19) with the astrophysical S value $S_{E2} = 20$ keV b. The result is given by the dashed line in Fig. 1. The nuclear amplitude was calculated from Eq. (20) using the formalism described in the text which follows it. The calculated curve is shown as a dash-dotted line in Fig. 1. The solid curve is the total cross section, including the interference between the nuclear and the Coulomb amplitudes. Both cross sections are strongly influenced by diffraction effects. The Coulomb cross section peaks at $\theta_a \approx 2°$. At lower angles, corresponding to collisions with large impact parameters, the Coulomb field is weak and the cross section is small. At large angles the Coulomb cross section decreases with increasing angle due to the strong absorption at small impact parameters. The nuclear cross section oscillates with a diffraction pattern which basically reflects the geometry of the system.

The total cross section is strongly influenced by the nuclear contribution to the breakup. A direct relationship between the breakup cross sections and the radiative capture cross sections seems to be infeasible at these bombarding energies. The Coulomb cross section at smaller values of E_{bc} is dominated by the nuclear breakup. However, a final judgement of the possible use of the Coulomb dissociation method for this reaction case should only be made after a microscopic calculation for the transition density from the ground state of ^{16}O to the $\alpha+^{12}C$ continuum is done. This is because the nuclear breakup is only sensitive to the tail of each wave function. The

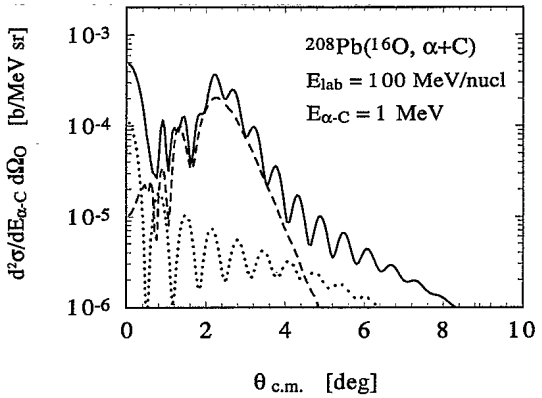

FIG. 1. Differential cross section for the breakup reaction $^{16}O+Pb \longrightarrow \alpha+^{12}C+Pb$ at 100 MeV/nucleon, with final relative energy of the fragments equal to 1 MeV, and as a function of the scattering angle. The dashed (dot-dashed) curve is due to the Coulomb (nuclear) breakup. The solid curve includes both mechanisms and the interference between them.

form of the tail might be reasonably well described by the two-body model used here. The internal part of each wave function is only relevant for an overall normalization. But this normalization is important to describe the magnitude of the wave function in the tail and this is very much dependent on the model assumed for the intrinsic structure of the $b + c$ system. As shown in Ref. [15] the internal structure of the α and ^{12}C are important to give the correct number of nodes in the ground state and continuum wave functions.

The situation is much better for the ^{8}B breakup. Since the binding energy of the p+^{7}Be system is very small, the Coulomb breakup amplitude is very large. This also changes the dependence of the Coulomb cross section on the bombarding energies. It is found that the total Coulomb breakup cross section is maximum at bombarding energies of order of 10 MeV/nucleon. In Fig. 2 we show the differential cross section for the breakup of ^{8}B at 50 MeV/nucleon and $E_{bc} = 100$ keV. The Coulomb amplitude is dominated by the $E1$ multipolarity. We used the value of $S_{E1} = 20$ eV b. One sees that for c.m. scattering angles smaller than 6° the cross section is dominated by the Coulomb interaction. The peak at very small angles reflects the fact that the large impact parameters contribute more to the cross section.

It is instructive to compare with the Coulomb cross section obtained with a semiclassical method [7]. In this case the equivalent photon number which enters in Eq. (12) is given analytically by

$$\frac{dn_{E1}}{d\Omega_a} = \frac{Z_A^2\alpha}{4\pi^2}\left(\frac{c}{v}\right)^2 \epsilon^4\,\zeta^2\; e^{-\pi\zeta}\left\{\frac{1}{\gamma^2}\,\frac{\epsilon^2-1}{\epsilon^2}\left[K_{i\zeta}(\epsilon\zeta)\right]^2 + \left[K'_{i\zeta}(\epsilon\zeta)\right]^2\right\}, \qquad (30)$$

where $\epsilon = 1/\sin(\theta_a/2)$, $\alpha = 1/137$, $\zeta = E_x a_0/\gamma\hbar v$, and $a_0 = Z_a Z_A e^2/2E_{\rm lab}$.

Using the above expression for $dn_{E1}/d\Omega_a$ in Eq. (11) we obtain the dashed curve in Fig. 3 for the same reaction, but at 30 MeV/nucleon. One observes that the quantum result deviates from the semiclassical one at $\theta > 4°$. At lower angles the agreement is quite good.

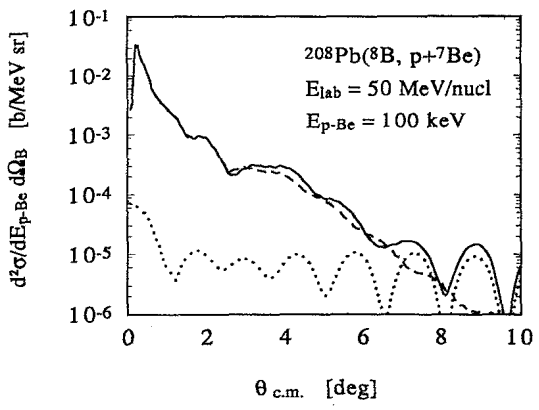

FIG. 2. Same as in Fig. 1, but for the reaction ^{8}B+Pb $\longrightarrow p$+^{7}Be+Pb at 50 MeV/nucleon and $E_{p\text{-Be}} = 0.1$ MeV.

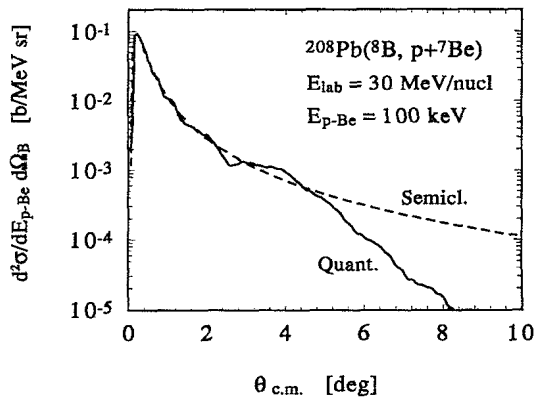

FIG. 3. Comparison between the angular distribution for the Coulomb breakup in Fig. 2 with another obtained by means of a semiclassical calculation (dashed curve).

This shows that strong absorption is not relevant for the scattering at low angles. The peak at small angles is a consequence of the adiabaticity condition. For $\zeta \gg 1$ ($\theta_a \ll 0.3°$) the Coulomb field is too weak to provide the necessary breakup energy. For $\zeta \ll 1$ ($\theta_a \gg 0.3°$) the Coulomb field is very strong and privileges the breakup of the projectile to final relative motion energies E_{bc} larger than 100 keV. Therefore, the cross section at a fixed relative energy of the fragments in the final channel has a peak at the optimal scattering angle corresponding to that energy. For the case above this angle is about 0.3°. We note that this is the angle for the scattering of the c.m. of the p+^{7}Be system. Due to the energy transfer, the fragments will be observed in a much larger opening angle, as we discuss in the next section.

An interesting problem is related to the excitation of the ^{7}Be fragments. ^{7}Be has an excited state at $E^* = 450$ keV. Since this energy is small, an appreciable amount of excited ^{7}Be fragments could be expected. But, since the virtual photon spectrum decreases with the photon energy this does not actually occur. From the equations developed in Sec. I one can show that the ratio between the cross sections for the two breakup possibilities is given by (assuming that the S factor for the capture from the excited state in ^{7}Be is the same as that for the ground state)

$$\frac{\sigma^*}{\sigma} = \frac{E_x^3}{(E_x+E^*)^3}\,\frac{n_{E1}(E_x+E^*)}{n_{E1}(E_x)}, \qquad (31)$$

where $n_{E1}(E_x)$ is the total virtual photon numbers for a ^{8}B+Pb collision [7]. We find that this ratio is less than 0.04 at collisions in the range of $E_{\rm lab} = 30 - 100$ MeV/nucleon.

V. ENERGY RESOLUTION AND REACCELERATION EFFECTS

Although the c.m. of the fragments are focused at small angles for a small energy transfer, there will exist an appreciable opening angle for the fragments. This opening angle can be obtained from Eq. (3). One gets

$$\frac{E_c}{m_c} = \left[\left(\frac{E_{bc}}{m_{bc}} - \frac{E_b}{m_b}\right) + 2\,\frac{E_b}{m_b}\,\cos^2\theta_{bc}\right] \pm \sqrt{\left[\left(\frac{E_{bc}}{m_{bc}} - \frac{E_b}{m_b}\right) + 2\,\frac{E_b}{m_b}\,\cos^2\theta_{bc}\right]^2 - \left(\frac{E_{bc}}{m_{bc}} - \frac{E_b}{m_b}\right)^2}\,, \tag{32}$$

where

$$\cos\theta_{bc} = \cos\theta_b\cos\theta_c + \sin\theta_b\sin\theta_c\cos(\phi_b - \phi_c)\ . \tag{33}$$

The plus (minus) sign in Eq. (32) corresponds to the solution when the fragment c is faster (slower) than fragment b, but having the same relative energy. Also, the above relation limits the values of θ_{bc} for which one has a real solution for E_c. One obtains that the following condition has to be fulfilled:

$$\cos^2\theta_{bc} \geq 1 - \frac{m_b}{m_{bc}}\,\frac{E_{bc}}{E_b}\ . \tag{34}$$

For the reaction ^{8}B+Pb at 50 MeV/nucleon, if we set $E_{\rm proton} = 50$ MeV, and $E_{bc} = 250$ keV, then $\theta_{\rm proton\text{-}^7Be}$ can be as large as 5°.

Also important is the uncertainty in E_{bc} due to the uncertainty in θ_{bc} and in E_b and E_c. From (3) one has

$$E_{bc} = m_{bc}\left[\frac{E_b}{m_b} + \frac{E_c}{m_c} - 2\sqrt{\frac{E_bE_c}{m_bm_c}}\,\cos\theta_{bc}\right]\ . \tag{35}$$

The resolution depends upon θ_{bc} via

$$\Delta E_{bc} = 2\,m_{bc}\sqrt{\frac{E_bE_c}{m_bm_c}}\,\sin\theta_{bc}\,\Delta\theta_{bc}\ . \tag{36}$$

The energy resolution which may be obtained is significantly better than the energy resolution of either detector telescope [4]. For example, in the reaction ^{8}B+Pb $\longrightarrow p$+^{7}Be+Pb at $E_{\rm lab} = 400$ MeV, taking $E_{\rm proton} = 50$ MeV, $E_{^7\rm Be} = 350$ MeV, $\theta_{bc} = 5°$, and $\Delta\theta = 0.1°$, we get $\Delta E_{bc} = 13$ keV.

In terms of velocities Eq. (35) reads

$$V_{bc}^2 = V_b^2 + V_c^2 - 2\,V_bV_c\cos\theta_{bc}\ . \tag{37}$$

An uncertainty in V_b results in

$$V_{bc}\,\Delta V_{bc} = V_b\,\Delta V_b - V_c\,\Delta V_b\cos\theta_{bc}\ . \tag{38}$$

The most favorable situation occurs when the nuclei decay perpendicular to the direction of motion. In such a case

$$V_c\cos\theta_{bc} \approx V_c \approx V_b\ , \tag{39}$$

and hence the right-hand side of (38) becomes small, i.e.,

$$V_{bc}\Delta V_{bc} \ll V_b\Delta V_b\ . \tag{40}$$

Similarly we can show that

$$V_{bc}\Delta V_{bc} \ll V_c\Delta V_c\ , \tag{41}$$

and the resolution which can be obtained depends weakly on the energy resolution for E_b and E_c. These results give support to the studies performed in Ref. [4] regarding the accuracy limits in determining E_{bc}. It is important to note that these arguments are valid when a reasonable energy resolution for the radioactive beam (in this case, a ^{8}B beam) is possible. Because of the poor quality of typical secondary beams, the energy resolutions might be much worse than those obtained above.

A last and more involved problem which one has to consider is the possible reacceleration of the fragments after the breakup. This occurs due to the action of the Coulomb field of the target. For fragments with equal charge-to-mass ratio, e.g., α and ^{12}C, the reacceleration is the same and no net effect is observed. On the contrary, e.g., p and ^{7}Be, there will be a deviation of the measured E_{bc} from the relative motion energy associated with the energy transfer in the breakup.

The final state interaction between the fragments is not relevant since this will also be manifest in the reverse radiative capture reaction of interest. What matters here is the further reacceleration of the fragments after the breakup. We will use the following procedure to calculate the reacceleration effect. We assume that the breakup occurs at the distance of closest approach and that the fragments follow Coulomb trajectories afterwards. We assume that the particles are separated by a distance of 4 fm at their initial breakup position. At the end of their trajectories the extra relative energy gained by reacceleration is determined. This will depend on their orientation at the breakup point. Thus, their initial orientation is taken randomly and the final result is averaged over the number of simulations. A similar method has been used in Ref. [16] to account for the reacceleration effect in ^{7}Li breakup experiments.

For p+^{7}Be incident on lead at 50 MeV/nucleon (solid curve) and 100 MeV/nucleon (dashed curve) the reacceleration energy is shown in Fig. 4 as a function of the impact parameter. It is large ($\sim$ 120 keV at 50 MeV/nucleon) at grazing impact parameters. But it decreases rapidly with increasing impact parameter. An initial relative energy is given to the fragments. But it is found that the dependence of the reacceleration effect on it is very small for the relative energies of interest, $\sim$ 100 keV.

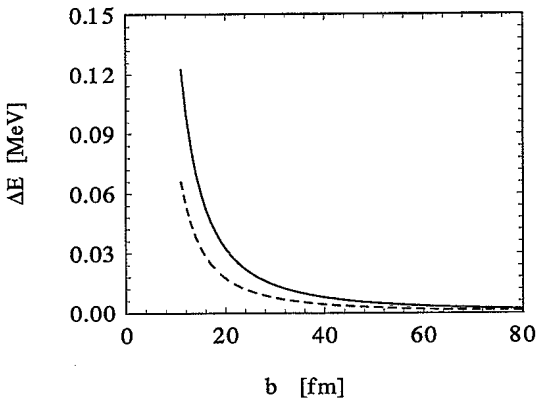

FIG. 4. Extra relative energy due to Coulomb reacceleration of the proton and ^{7}Be after the breakup.

The reacceleration energy for a given impact parameter has to be weighted with the breakup probability:

$$\langle \Delta E \rangle = \int_{b_{\min}}^{\infty} d^2b\, P(b)\, \Delta E(b) \Big/ \int_{b_{\min}}^{\infty} d^2b\, P(b)\ . \tag{42}$$

This quantity does not depend on the model for the nuclear breakup since the excitation probability is a product of kinematical factors and the matrix elements for the breakup [7]. These matrix elements do not depend on b and are cancelled in the division. Using the analytical formulas obtained in the semiclassical theory [7] one gets

$$\langle \Delta E \rangle = \int_{b_{\min}}^{\infty} d^2b \left[K_1^2(\xi) + K_0^2(\xi)/\gamma^2\right] \Delta E(b) \Big/ \int_{b_{\min}}^{\infty} d^2b \left[K_1^2(\xi) + K_0^2(\xi)/\gamma^2\right], \tag{43}$$

where $\xi = E_x b/\hbar\gamma v$. Using $b_{\min} = 1.2(A_a^{1/3} + A_A^{1/3})$ fm and the results obtained above for $\Delta E(b)$ we find $\langle \Delta E(b) \rangle = 14.6$ keV and 9.3 keV for $E_{\rm lab} = 50$ and 100 MeV/nucleon, respectively. These values are tolerable for the precision that one wants to extract from the experiments.

VI. CONCLUSIONS

The possibility of using the Coulomb dissociation method to determine the radiative cross sections $\alpha(^{12}\mathrm{C}, \gamma)^{16}\mathrm{O}$ and $p(^7\mathrm{Be}, \gamma)^8\mathrm{B}$ has been investigated. While the perspectives are not very favorable for the former reaction, they are quite good for the later one. This is basically due to the very small binding of ^{8}B which renders a very large Coulomb dissociation cross section. The nuclear contribution to this reaction is negligible for scattering to forward directions.

The limits of energy resolution that one may extract from these experiments were also investigated. The method limits the energy resolution for the radiative capture energy in the range of 10–20 keV. Therefore, experiments using this method for the $p(^7\mathrm{Be}, \gamma)^8\mathrm{B}$ are promising and should be encouraged.

The perspectives of using this method for other reactions of astrophysical interest depend essentially on the energy transfer required. For loosely bound systems, e.g., ^{8}B, the Coulomb force is very effective to induce the breakup and the Coulomb cross section can be many orders of magnitude larger than the nuclear one for properly chosen experimental conditions. On the other hand, experiments with stable beams, e.g., ^{16}O, benefits from the intensity of the beam which can be obtained with many orders of magnitude higher than that for a radioactive beam, e.g, ^{8}B. One could sacrifice a great deal in magnitude of the cross section if an energy could be found at which the nuclear contribution would be negligible. To obtain a definite answer to this question more theoretical effort is certainly needed.

I am very indebted to Sam Austin, Moshe Gai, and Tohru Motobayashi for stimulating discussions.

[1] B.W. Filippone, J. Humblet, and K. Langanke, Phys. Rev. C **40**, 515 (1985).
[2] L. Buchmann *et al.*, Phys. Rev. Lett. **70**, 726 (1993).
[3] Z. Zhao *et al.*, Phys. Rev. Lett. **70**, 2066 (1993).
[4] G. Baur, C.A. Bertulani, and H. Rebel, Nucl. Phys. **A458**, 188 (1986).
[5] T. Motobayashi *et al.*, Phys. Lett. B **264**, 259 (1991).
[6] J. Kiener *et al.*, Phys. Rev. C **44**, 2195 (1991).
[7] C.A. Bertulani and G. Baur, Phys. Rep. **163**, 299 (1988).
[8] T.D. Shoppa and S.E. Koonin, Phys. Rev. C **46**, 382 (1992).
[9] C.E. Rolfs and W.S. Rodney, *Cauldrons in the Cosmos* (University of Chicago Press, Chicago, 1988).
[10] G. Baur and M. Weber, Nucl. Phys. **A504**, 352 (1989).
[11] C.A. Bertulani and A.M. Nathan, Nucl. Phys. **A554**, 158 (1993).
[12] M.S. Hussein, R.A. Rego, and C.A. Bertulani, Phys. Rep. **201**, 279 (1991).
[13] S.M. Lenzi, A. Vitturi, and F. Zardi, Phys. Rev. C **40**, 2114 (1989).
[14] C.W. de Jager *et al.*, At. Data Nucl. Data Tables **14**, 479 (1974).
[15] K. Langanke and S.E. Koonin, Nucl. Phys. **A410**, 334 (1983); **439**, 384 (1985).
[16] J.E. Mason, S.B. Gazes, R.B. Roberts, and S.G. Teichmann, Phys. Rev. C **45**, 2870 (1992).